Myocardial Extraction of 1-[^{11}C] Betamethylheptadecanoic Acid

David R. Elmaleh, Eli Livni, Nathaniel M. Alpert, H. William Strauss, Richard Buxton and Alan J. Fischman

Division of Nuclear Medicine, Department of Radiology, Massachusetts General Hospital and Department of Radiology, Harvard Medical School, Boston, Massachusetts

Betamethylheptadecanoic acid (BMHA) is a branched chain fatty acid analog that is transported into myocardial cells by the same long chain fatty acid carrier protein mechanism as natural fatty acids, but cannot be completely catabolized and accumulates in the tissue. Thus, ^{11}C-labeled BMHA is a useful tracer for the noninvasive evaluation of myocardial fatty acid utilization by positron emission tomography (PET). **Methods:** As a prelude to PET studies, the metabolism of BMHA was studied by classical techniques. We measured the net extraction fraction (E$_n$) of 1-[^{11}C]-beta-R,S-methylheptadecanoic acid (1-[^{11}C]BMHA) and compared it to that of natural fatty acids in dogs, using arterial/venous measurements and a mathematical model. Two groups of conditioned dogs were studied. In the first group, measurements were made under fasting (normal control) conditions and in the second group, measurements were made during glucose and insulin infusion. Myocardial blood flow, and the extraction/utilization of other substrates (glucose, oxygen and lactate) were also measured. **Results:** For natural fatty acids in the basal state, E$_n$(FA) was 0.335. After glucose/insulin infusion, this value decreased to 0.195. The 1-[^{11}C]BMHA showed a similar decrease in E$_n$(BMHA) from 0.220 in the control group to 0.100 in the group treated with glucose/insulin infusion. Preliminary PET studies with 1-[^{11}C]BMHA verified the validity of performing these measurements noninvasively. **Conclusion:** The results of these studies indicate that rates of fatty acid metabolism in the myocardium can be determined from steady-state concentrations of 1-[^{11}C]BMHA.

Key Words: fatty acids; myocardium; PET; betamethylheptadecanoic acid; metabolism

R adionuclide imaging of myocardial perfusion and ventricular function are useful for identifying areas of ischemia and defining its impact on global and regional function. Although these measurements usually provide complementary data in patients with stable coronary artery disease (1,2), situations occur where the information is inconsistent. The fact that about 20% of patients with "fixed" thallium defects have ischemia (3–5) challenges the utility

of thallium imaging for defining zones of ischemia. Perfusion and function are discordant immediately after thrombolysis (6,7) and in some patients with cardiomyopathy (8,9). These observations suggest that in addition to perfusion and function, other measurements are needed to characterize the ischemic myocardium. Studies by Schelbert (10) and Schwaiger et al. (11) have shown that a mismatch between glucose utilization and perfusion determined by positron emission tomography (PET) is a sensitive indicator of ischemic but viable myocardium.

Fatty acids (FAs) are the major source of energy for the myocardium (12–15). In plasma, FAs are transported bound to albumin and diffuse through the capillary wall and sarcolemma (16,17). This process may be active or passive (18). The entry of FA into tissue depends upon: (1) chain length; (2) the presence of double bonds and side chains; (3) blood flow to the myocardium; (4) the concentration of FA in plasma and (5) the metabolic state of the myocardium. Once in the cell, FAs undergo oxidative metabolism (16) or are incorporated into triglycerides (TG). Based on these properties, it is predicted that a depression of FA extraction and/or oxidation will occur in zones of myocardial ischemia or infarction. Thus, FA imaging could supplement the results of studies of perfusion and glucose metabolism in the evaluation of myocardial injury. For example, after injury, baseline FA imaging could be used to define the state of myocardial metabolism and after intervention or medical therapy, follow-up imaging could be used for monitoring the resumption of oxidative metabolism.

The use of ^{11}C-palmitic acid (1-[^{11}C]PA) as a positron emitting "physiological" substrate was proposed by Klein (19), Weiss (20), Schon (21) and Schelbert (22). Their studies and others (19,23–31) provide the experimental basis for quantifying myocardial FA metabolism with 1-[^{11}C]PA and PET. However, the rapid blood clearance of these tracers and loss of radioactivity from myocardial tissue due to straight chain FA catabolism by beta oxidation significantly complicates data analysis.

Previously, we proposed the use of beta-methylheptadecanoic acid (BMHA) for evaluating myocardial FA metabolism (27). The use of this modified FA may overcome some of the problems associated with straight chain FA. We have shown that BMHA enters myocardial cells by the

same mechanism as unbranched FA, accumulates in the same metabolic compartments and that its subcellular distribution in mitochondria and lipid droplets mimics that of natural FA. Although one report indicated that a significant amount of 1-[^{11}C]-beta-methylheptadecanoic acid (1-[^{11}C]BMHA) is metabolized to CO_2, in the animal preparation that we used, myocardial and hepatic metabolism could not be isolated (32). In contrast, recent studies with isolated perfused rat hearts have demonstrated negligible CO_2 production (33). Thus, this compound appears to act as a true FA analog that is partially metabolized and retained in myocardial cells (34,35).

To investigate the utility of BMHA as a tracer for quantifying FA metabolism by PET, we compared the net extraction fraction (E_n) of 1-[^{11}C]BMHA to that of natural FA in dogs, using arterial/venous measurements and a mathematical model. Two groups of conditioned dogs were studied. In the first group, measurements were made under fasting (normal control) conditions and in the second, group, measurements were made during glucose and insulin infusion.

E_n(FA) for natural FA was 0.335 in the control state and decreased to 0.195 after glucose/insulin glucose infusion. 1-[^{11}C]BMHA showed a similar decrease in E_n(BMHA) from 0.220 in the control group to 0.100 in the group treated with glucose/insulin infusion. Myocardial blood flow, and the extraction/utilization of other substrates (glucose, oxygen, and lactate) were also measured.

METHODS

Radiopharmaceuticals

Carbon-11-BMHA was prepared according to a previously reported procedure (27). Typically, specific activity was ~200 mCi/mmole and radiochemical purity was >99%. 1-[^{14}C]BMHA was purchased from Amersham Inc. (Arlington Heights, Il). The ^{113}Sn microspheres were purchased from New England Nuclear Corp. (Billerica, MA).

Animal Preparation

Conditioned mongrel dogs weighing 20 to 25 kg were used in all experiments. The animal protocol was approved by the Massachusetts General Hospital animal care committee. The dogs were maintained on a Wayne Promix standard diet dog chow for 3 to 7 days. The animals were placed on a fast 12 hr prior to the study. Groups of 6–8 dogs were used in all experiments.

The dogs were anesthetized with sodium pentobarbital (25 mg/kg), intubated and ventilated with room air using a Harvard respirator. A catheter was placed in the aorta for monitoring systemic blood pressure and for withdrawal of arterial blood samples. A catheter was placed in the jugular vein for administration of 1-[^{11}C]BMHA. A left thoracotomy was performed, and catheters were placed in the left atrium for injection of microspheres and in the coronary sinus for withdrawal of venous blood draining the myocardium. Arterial and coronary-sinus blood samples were assayed for glucose, oxygen, pH, lactic acid, pO_2 and pCO_2 to document that steady-state conditions were established before the injection of 1-[^{11}C]BMHA. Arterial and coronary sinus levels of FA were also determined; however, for logistical reasons these assays were performed after the study, on blood samples that were stored on ice. The blood sampling and metabolite measure-

ments were also performed 15 and 60 min after injection of 1-[^{11}C]BMHA.

1-[^{11}C]BMHA Kinetics in Dogs Placed on a Fast

Approximately 2 to 7 mCi of 1-[^{11}C]BMHA was injected intravenously and 0.5 ml of blood was withdrawn from the arterial and the coronary-sinus catheters and placed on ice for subsequent counting. Subsequent blood samples were then drawn every 3–5 sec for the first 10 min and every 5 min thereafter until 60 min had elapsed. At 60 min, myocardial blood flow was measured using the arterial reference technique with 2 × 10^6 ^{113}Sn-labeled microspheres.

After injection of the microspheres, the animals were killed by an injection of KCl and the hearts were quickly removed and sectioned into pieces weighing approximately 1 g. The tissue samples were placed into preweighed counting vials and ^{11}C radioactivity was measured. Also, the blood samples containing 1-[^{11}C]BMHA were assayed for carbon-11 activity. On the following day, ^{113}Sn radioactivity was measured, and the average blood flows to the whole myocardium, the left ventricle, the right ventricle and the septum were calculated. Arterial/venous differences in the FA levels were determined at baseline and 60 min postinjection. FA concentrations were determined using a NEFA kit.
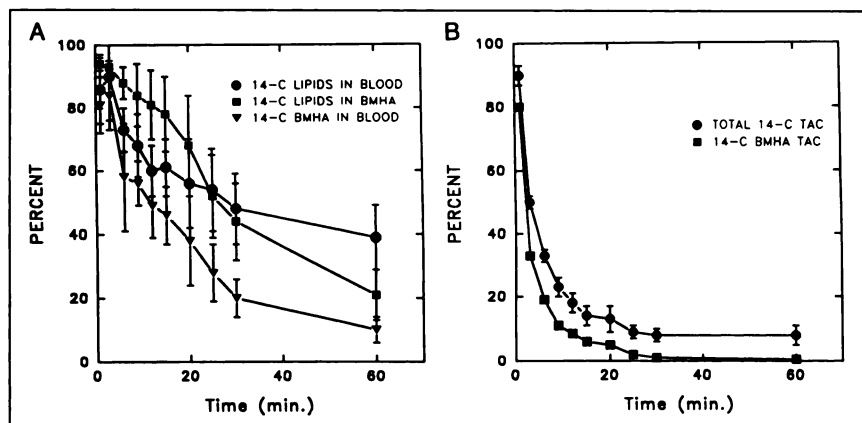
1-[^{11}C]BMHA Kinetics in Dogs During Glucose/Insulin Infusion

In another group of dogs, the glucose/insulin infusion schedule described by Schelbert et al. (22) was used. Fifty grams of dextrose and 200 U of insulin were added to 500 ml of water and the solution was infused over 90 min. The measurements described above were started 60 min after the start of the infusion.

Blood Time-Activity Curves for 1-[^{14}C]BMHA

Another group of dogs was anesthetized, intubated and ventilated with room air as described above. Arterial and venous lines were placed for blood sampling and injection of 1-[^{14}C]BMHA. After intravenous injection of approximately 2 mCi of 1-[^{14}C]BMHA, arterial blood samples were collected at 3, 6, 9, 12, 15, 20, 25 and 30 min. The percentage of the total radioactivity in blood that was associated with lipids was measured as follows. The blood samples were centrifuged and plasma (0.5 ml) was shaken with 2.5 ml of isopropanol:heptane: 1.0 N H_2SO_4, (40:10:1) for 10 min. Heptane (1.5 ml) and H_2O (1 ml) were added and the mixture was shaken briefly. The layers were separated and their volumes were measured. Aliquots (0.1 ml) of the upper (lipid) and lower (aqueous) layers were transferred to scintillation vials, ^{14}C radioactivity was measured and the percentage of the total radioactivity in the lipid layer was calculated. Determination of the contribution of 1-[^{14}C]BMHA to total lipid radioactivity was performed as follows: Aliquots (1.0 ml) of the upper layer were evaporated to dryness, and the residue was dissolved in $CHCl_3$ (0.2 ml). Ten 1-μl aliquots of the solutions were analyzed by TLC on silica gel plates (60 F254, 0.2 mm on aluminum) using the solvent system; hexanes:ether:acetic acid, 50:50:1. The plates were scanned with a Bioscan Radiochromatogram Analyzer (Bioscan Inc., Washington, DC) and the fraction of the total radioactivity that migrated at the position of BMHA was calculated. Corrected time-activity curves for 1-[^{14}C]BMHA in blood were derived from: the total carbon-14 radioactivity in blood, the percentage of carbon-14 radioactivity that was associated with lipids and the contribution of 1-[^{14}C]BMHA to total lipid radioactivity. Analogous methods were used to derive corrected time-activity curves for 1-[^{11}C]BMHA in blood. These curves were used for kinetic modeling.

FIGURE 1. (A) Time dependence of the percentage of the total radioactivity in blood that is associated with lipids; the percentage of total lipid-associated radioactivity that is present as BMHA (determined by TLC) and the percentage of total blood radioactivity that is present as 1-[^{14}C]BMHA. (B) Time-activity curves for total ^{14}C in blood and the corrected 1-[^{14}C]BMHA curve. The latter curve was derived by multiplying the curves for total ^{14}C radioactivity in blood and the percentage of total blood radioactivity that is present as 1-[^{14}C]BMHA. Each point is the mean ± s.d. for 6–8 animals.

PET Measurements

Images were acquired with a PC-384 PET camera (Scanditronix AB, Sweden) (36). The primary imaging parameters of this instrument are an in-plane resolution of 7.0 mm FWHM, an axial resolution of 12 mm FWHM, five contiguous slices of 14 mm separation and a sensitivity of ~22,000 cps/μCi.

The dogs were placed supine on a Plexiglass imaging cradle with the heart oriented so that the central imaging plane transversed the mid-left ventricle perpendicular to its long axis. A transmission image for attenuation correction was recorded using a cylindrical annulus containing a solution of ^{68}Ga. Two to 6 mCi of 1-[^{11}C]BMHA was then injected intravenously and serial PET images were acquired every 10 sec for 9 min and then every minute for a total imaging time of 30 min.

All images were reconstructed using a conventional filtered back-projection algorithm to an in-plane resolution of 7 mm FWHM. The projection data were corrected for nonuniformity of detector response, dead time, random coincidences and scattered radiation. Circular regions of interest (fixed diameter of 16 mm) were drawn over the myocardium and the left ventricular blood pool. The PET camera was cross-calibrated against a well scintillation counter by comparing the PET camera response from a ^{68}Ga solution in a 20-cm cylindrical phantom with the response of the well counter to an aliquot of the same solution.

Data Analysis

Kinetic parameters of BMHA uptake were determined for each study condition using the operational equation described in the Appendix. Our guiding hypothesis is that there is a reproducible relationship between the net extraction fractions of FA and BMHA. Assuming that uptake and metabolism of native FA is in a steady state, the rate of metabolism (R) can be described by the Fick equation:

$$R = E_n * F * C_a \; (\mu\text{mole/min/g}), \qquad \text{Eq. 1}$$

where E_n = net extraction fraction; F = blood flow (ml/min/g) and C_a = arterial concentration of FA (μmole/ml).

In the modeling calculations, we have made use of the assumption that, at steady state, the rate at which FA leaves the tissue through oxidation must equal the rate at which FA enters from the blood. The net extraction of a substrate metabolized by the heart at steady state can be determined from the arterial and coronary sinus concentrations. If there is a simple relationship between net extraction of BMHA and natural FA, measurements of E_n(BMHA) can be used to calculate E_n(FA). In the present stud-

ies, we tested the validity of the assumption that this relationship can be described as a constant ratio:

$$L = E_n(\text{FA})/E_n(\text{BMHA}), \qquad \text{Eq. 2}$$

with L playing the same role as the "lumped" constant in the Sokoloff model for deoxyglucose metabolism. If L is independent of myocardial blood flow, free FA concentration and composition and other physiological mechanisms, then the rate of FA metabolism (R) can be calculated from measurements of E_n(BMHA). To perform these calculations, myocardial blood flow was calculated from microsphere data by the method of Heymann et al. (34) and corrected 1-[^{11}C]BMHA blood curves were calculated from the 1-[^{11}C]BMHA blood curve and the metabolic fate of 1-[^{14}C]B-MHA in blood as described above. The BMHA time-activity curves were integrated using a cubic spline numerical integration procedure to give the cumulated BMHA activity as a function of time. This integral (I), the 1-[^{11}C]BMHA concentration from time zero to 1 hr ([BMHA]), and the myocardial blood flow (F) were used to calculate the net extraction fraction for BMHA (E_n(BMHA)) using the relationship:

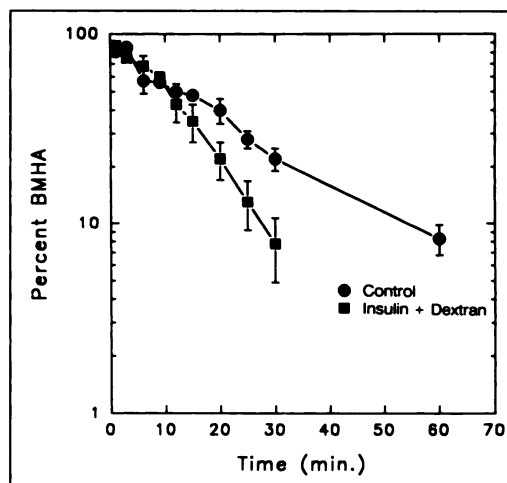$$E_n(\text{BMHA}) = [\text{BMHA}]/(F * I). \qquad \text{Eq. 3}$$

FIGURE 2. Corrected time-activity curves for 1-[^{11}C]BMHA in control and insulin/dextrose treated dogs. Each point is the mean ± s.d. for 6–8 animals.

TABLE 1
Arterial and Venous pCO_2 and pH of Dogs in the Control State

	Arterial		Venous	
	10 min	15 min	10 min	15 min
pCO_2	38.34 ± 8.24	35.32 ± 30.9	44.99 ± 9.92	43.00 ± 1.78
pH	7.36 ± 0.07	7.34 ± 0.10	7.30 ± 0.06	7.30 ± 0.10

The value of I at 15 min and at 1 hr differed by less than 10% in all experiments.

RESULTS

Blood Time-Activity Curve Following Intravenous Injection of 1-[^{11}C]BMHA and 1-[^{14}C]BMHA

The quantitative evaluation of BMHA utilization rate depends upon knowledge of the correct input function from arterial blood to myocardium. In a series of dogs injected with 1-[^{14}C]BMHA, the lipid and aqueous fractions of blood were analyzed for ^{14}C activity at multiple time points. Figure 1A shows the time dependence of the percentage of the total radioactivity in blood that was associated with lipids; the percentage of total lipid associated radioactivity that is present as BMHA (determined by TLC) and the percentage of total blood radioactivity that is present as 1-[^{14}C]BMHA. Figure 1B shows the time-activity curves for total ^{14}C in blood and the corrected 1-[^{14}C]BMHA curve. The latter curve was derived by multiplying the curves for total ^{14}C radioactivity in blood and the percentage of total blood radioactivity that is present as 1-[^{14}C]BMHA. As expected, 1-[^{14}C]BMHA concentration approached zero at the later time points. Figure 2 shows BMHA time-activity curves calculated for dogs in the basal state (12-hr fast) and during glucose/insulin infusion. These curves were used to calculate the blood integrals for kinetic modeling.

Net Extraction Fraction Measurements

Table 1 shows the average arterial and venous pCO_2 and pH in dogs at 10 and 15 min after tracer administration. Table 2 presents the calculated net extraction fractions for 1-[^{11}C]BMHA, FA, glucose and lactate and the myocardial blood flow. The measured myocardial concentrations for these substrates are shown in Table 3. Table 4 summarizes the mean calculated utilization rates of these substrates in the basal state and following the infusion of glucose/insulin.

The net extraction fraction of BMHA decreased from 0.22 in the control state to 0.100 after glucose/insulin infusion (decrease of ~45%). This decrease was similar to the change in natural free FA net extraction, from 0.35 to 0.19 (decrease of ~54%). Similarly, the utilization rate of 1-[^{11}C]BMHA decreased from 0.062 μmole/min/g (control) to 0.016 μmole/min/g (glucose/insulin) (~75% decrease) and was proportional to the decrease in natural free FA utilization (from 0.098 μmole/min/g to 0.020 μmole/min/g, ~80% decrease).

The ratio of the net extraction fractions of BMHA and

natural free FA (an indicator of the magnitude of the lumped constant) was slightly lower in glucose/insulin-treated dogs compared to control animals (0.53 versus 0.63). However, this difference was not statistically significant.

PET Imaging

Five dogs were studied by serial PET imaging. Prolonged retention of 1-[^{11}C]BMHA was demonstrated in all animals. Figure 3 shows the time-activity curve for 1-[^{11}C]BMHA in the myocardium of one animal after correction for the contribution of ^{11}C tracer in the blood. The solid line represents a least-squares fit of the kinetic model to the PET data. The tissue curve demonstrates that after an initial uptake phase, myocardial concentration of 1-[^{11}C]BMHA reaches a plateau within about 15 min and remains at this level for the remainder of the experiment. Since, microsphere flow was also measured in this study, we computed a model-independent estimate of net BMHA extraction according to Equation 3, yielding a value of $E_n = 0.29$, which is in reasonable agreement with the values determined by direct tissue radioactivity measurements. Figure 4 shows a series of transaxial PET images of the heart of a dog injected with 5.0 mCi of 1-[^{11}C]. These images represent the average concentration from 15 to 30 min after injection. Since the tracer is retained in triglyceride pools as the "SCoA form," image quality is excellent.

DISCUSSION

The myocardium can utilize lactate, acetate, FA and glucose to satisfy its contractile energy needs. Under aerobic circumstances, most of the energy for ATP production is provided by the complete oxidation of FA or glucose (depending on blood glucose and insulin levels) to carbon dioxide and water. These products of catabolism are diffusible and are carried away from the myocyte as they are produced when blood flow is adequate. When blood flow is significantly reduced, tissue delivery of oxygen and removal of waste products are reduced. As a result, oxygen-

TABLE 2
Net Myocardial Substrate Extraction Fraction in Dogs Under Control Conditions and with Glucose/Insulin Infusion

	Net E_f*	
Substrate	Control	Glucose/Insulin[†]
Oxygen	0.56 ± 0.14[‡]	0.44 ± 0.048
Glucose	0.10 ± 0.10	0.028 ± 0.054
Lactate (10 min)	0.56 ± 0.22	0.49 ± 0.09
Free Fatty Acids	0.35 ± 0.12	0.193 ± 0.077
[^{11}C]BMHA	0.22 ± 0.11	0.100 ± 0.049

*Net E_f, mean ± s.d.
[†]Since net extraction measured by Schelbert et al. (22) refers to the unidirectional extraction fraction, comparisons were not made.
[‡]Myocardial blood flow: 1.31 ± 0.66 ml/min/g (n = 6, control), 2.26 ± 0.90 ml/min/g (n = 6, glucose/insulin).

TABLE 3

TABLE 3
Myocardial Substrate Concentrations in Dogs Under Control Conditions and with Glucose/Insulin Infusion

	Current Study			Literature*	
Substrate	Control	Glucose/ Insulin	Ratio	Control	Glucose/ Insulin
FFA (mEq/liter)	0.21 ± 0.11	0.07 ± 0.03	3	0.39 ± 0.15	0.20 ± 0.97
Glucose (mEq/g)	89.6 ± 10.5	204 ± 58	0.43	73.8 ± 2.25	192.7 ± 48.28
Oxygen (ml/ml)	0.19 ± 0.04	0.15 ± 0.01	1.19	NR	NR
Lactate (mmole/l)	1.41 ± 0.82	1.60 ± 0.46	0.88	1.03 ± 1.03	2.43 ± 0.96

*Schelbert et al. (22).
Values are mean ± s.d.
NR = not reported.

dependent substrate catabolism decreases. Since FAs are catabolized by beta oxidation to acetyl CoA, which requires the Krebs cycle, and ultimately oxidative phosphorylation to produce ATP, FA consumption ceases with anoxia (14).

Two general methods could be used to study myocardial metabolism in vivo: (1) the use of radiolabeled "natural" substrates such as [11C]glucose or 1-[11C]PA); or (2) the use of a well-designed metabolic analog such as 1-[11C]BMHA. The first approach using [11C]glucose or [11C]PA has an advantage since transport and metabolism of the radiopharmaceutical are identical to that of the natural substrates used by the tissue, and toxic effects should not be observed. The beta-oxidation metabolic process involves the alternating action of dehydrogenase and hydratase enzymes (Fig. 5). Acetyl-SCoA either returns to the cytoplasm and is used in various synthetic reactions (13,14) or enters the Krebs cycle to produce carbon dioxide and water. The oxidative process is repeated for a varying number of cycles, depending on the FA chain length. The scheme in Figure 6 illustrates the complexity of defining the intracellular kinetics of a substrate like ^{14}C- or ^{11}C-

labeled palmitic acid by autoradiography or PET, independent of the position on substrate labeling.

The second approach involves the use of an analog whose in vivo behavior is very similar to the FA from which it was derived. This analog should enter the same metabolic pathway as the natural substrate, however, at an early metabolic step, it should be trapped in a known form (1-[11C]BMHA) (Fig. 6) in a similar manner to 2-deoxyglucose and 2-fluoro-2-deoxyglucose. 1-[11C]palmitic acid is subject to the loss of the label as $R^{14}COSCoA$ or as $^{14}CO_2$ during the degradation steps of the FA beta-oxidation (Fig. 5). In contrast, 1-[C-11]BMHA is trapped in tissue because it cannot be converted to the corresponding 3-ketoacylS-CoA derivative (Fig. 6). The alpha and omega oxidation alternative pathways for FA metabolism are slow and make only a small contribution to FA metabolism. Recently, it was demonstrated that perfused hearts catabolize less than 5% of 1-[C-11]BMHA by alpha and omega oxidation over 2 hr (35).

A potential problem with the use of BMHA to study myocardial metabolism is the possibility that it is metabolized to other compounds in the circulation and these ra-

TABLE 4
Myocardial Substrate Utilization in Dogs Under Control Conditions and with Glucose/Insulin Infusion

	Current Study		Literature*	
Substrate	Control	Glucose/ Insulin	Control	Glucose/ Insulin
Flow (ml/min/g)	1.31	2.27	NR	NR
MR_{O2} (μmole/min/g)	6.50	7.02	NR	NR
MR_{Glu} (μmole/min/g)	0.34	0.37	1.19	0.50
MR_{Lac} (μmole/min/g)	1.03	1.78	NR	NR
MR_{FFA} (μmole/min/g)	0.098	0.020	0.10	0.024
MR_{BMHA} (μmole/min/g)	0.062	0.016	NR	NR

*Schelbert et al. (22).
Values are mean ± s.d.
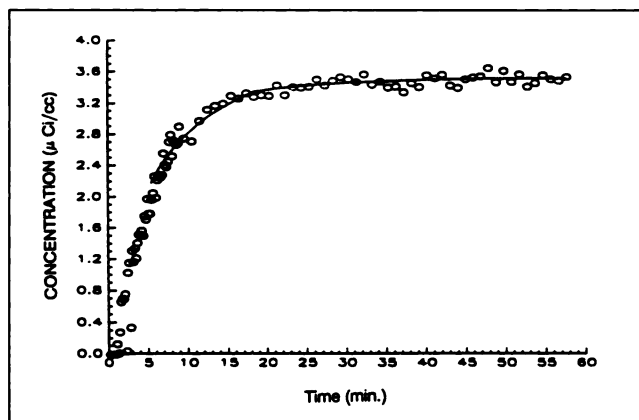NR = not reported.

FIGURE 3. Time dependence of the concentration of 1-[11C]B-MHA in the myocardium of a dog measured by PET (filled circles) after injection of 5.0 mCi of 1-[11C]BMHA. The solid curve indicates the least squares fit of the data to the proposed kinetic model.

FIGURE 4. Transaxial PET images of the heart of a dog injected with 5.0 mCi of 1-[^{11}C]BMHA. The data were acquired from 10 to 30 min after injection.

FIGURE 6. Schematic diagram of the metabolic compartments for transport and metabolism of BMHA.

diolabeled metabolites act as substrates for the myocardium. Studies with isolated rat liver preparations perfused with unlabeled BMHA revealed the evolution of 3-methylglutarate as well as a small amount of an unidentified metabolite (*31*). Also, the ^{11}C time-activity curves did not approach zero (Fig. 1). This observation may be explained by the presence of labeled metabolites in the blood. However, the possibility of significant myocardial uptake of these metabolites seems unlikely, since our studies in more than 20 dogs clearly show that following injection of 1-[^{11}C]BMHA, the A-V difference of plasma radioactivity tends toward zero within 10 to 12 min.

The measurements of myocardial metabolism reported here are in good agreement with previously reported results using ^{11}C-labeled palmitic acid. Tables 3 and 4 contain a comparison of our data for blood flow and metabolic utilization rates to the results of a previous report by Schelbert et al. (*22*, the data in this reference have been converted to the units used in the present study). Although in Schelbert's studies, metabolic measurements were made after intraarterial injection of the labeled "natural" FA 1-[^{11}C]PA, whereas our results were obtained after intravenous injection, the results should be the same. In both

studies, the calculated ratio of FFA:lactate:glucose utilization remained constant at 23:3:6 for both the control and glucose/insulin infusion groups. This ratio is derived from the equivalents of oxygen needed for converting the different molecules to water and CO_2. Overall, the marked similarity between the results of the two studies demonstrates a clear correlation between 1-[^{11}C]BMHA and 1-[^{11}C]PA metabolism.

The preliminary PET studies clearly demonstrate that 1-[^{11}C]BMHA can be used to evaluate myocardial FA uptake noninvasively. Although there was good agreement between E_n(BMHA) determined by PET and tissue radioactivity measurements, more reliable results could be obtained by measuring myocardial blood flow by PET.

CONCLUSIONS

The results obtained in an open-chest dog model using 1-[^{11}C]BMHA as a FA metabolic tracer validate the usefulness of 1-[^{11}C]BMHA for evaluating myocardial metabolism in both the fasting basal state and an altered state of increased glucose availability. The FA utilization rates measured with 1-[^{11}C]BMHA are proportional to those obtained from direct A-V difference measurements of natural FA. Also, our results are similar to previously reported data using 1-[^{11}C]PA. Other experiments must be performed to confirm the similarity of 1-[^{11}C]BMHA to the natural substrate in different physiological states of blood flow, myocardial work and oxygen availability. Also, these comparisons have to be made in different disease states. Overall, the results indicate that 1-[^{11}C]BMHA is a useful metabolic tracer for quantifying FA metabolism.

APPENDIX

Kinetic Model for BMHA Utilization

We make use of the working hypothesis that BMHA behaves like a native FA up to the beta-oxidation steps in the mitochondria where it is assumed to be sequestered for a long period of time as the beta-hydroxy-betamethyl acyl-SCoA form (Fig. 6). Highly
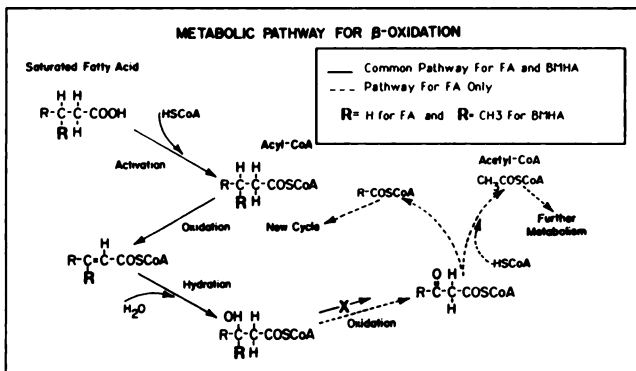

FIGURE 5. Schematic representation of the beta oxidation metabolic pathway. The solid arrows indicate metabolic reactions that are common to natural straight chain FA and BMHA. The dashed arrows indicate metabolic reactions that are restricted to natural FA.
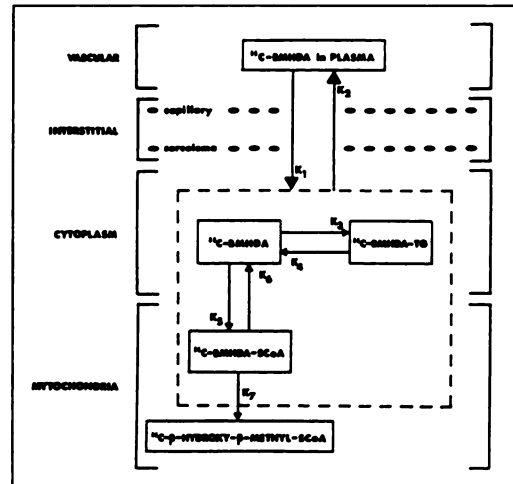
simplified, the fate of a FA may be described as follows: FA passes from capillary blood into the interstitial space. It may "backdiffuse" to the vascular space or continue forward passing through the sarcolemmal barrier. Once inside the cell, the FA may return to the interstitial space or may become activated as acyl-CoA. The activated FA can then be esterified to form triglycerides, incorporated into phospholipids or carried into the mitochondria and oxidized. The activation of FFA to acyl-CoA requires energy and is believed to be essentially irreversible in vivo. Since acyl-CoA cannot escape through the cell membrane, it is trapped in the cell until it reacts as described above. However, the formation of triglycerides is not irreversible and these can be broken down into the constituent FA and glycerol, adding to the FFA pool.

Based on the available evidence, BMHA cannot undergo beta-oxidation, and hence, is either trapped in mitochondria or incorporated into the triglyceride pool. The triglyceride pool turns over very slowly, as indicated by measurements with palmitic acid and now with BMHA. With respect to BMHA, as shown in Figure 3, the concentration of BMHA in myocardial tissue, following intravenous injection, reaches a plateau after 10–15 min. The simplest model consistent with the measured tissue curves and the biochemical data is one in which tissue is described by two compartments, a precursor FFA pool and a metabolically trapped pool, both driven in response to the BMHA concentration in the blood plasma.

Since BMHA cannot undergo beta-oxidation and because the turnover rate for the triglyceride pool is slow, the plateau of the tissue curve reflects both components. Measurements with BMHA can only determine the rate at which BMHA passes through the committed step to acyl-CoA. Accordingly, we can measure the steady state rate for incorporation into triglyceride plus beta-oxidation. This situation is analogous to the result that would be obtained if we could make Fick-type A-V measurements with a native FA such as palmitate.

Based on the considerations outlined above, we have derived an operational equation capable of describing the PET measurements in terms of the blood flow, F; the unidirectional extraction fraction, E; the net extraction fraction, E_n and the rate, K that BMHA is cleared from the "precursor pool." The rate constant K is the sum of two rates: K_2, the rate of back-diffusion, and K_3, the rate of activation of BMHA to the CoA form. Neglecting tracer in blood, the operational equation is given as:

$$C(t) = F * [(E - E_n) * Exp(-K * t) + E_n](*)C_a(t),$$

where C(t) is the tissue concentration at time t, $C_a(t)$ is the plasma concentration at time t and (*) represents the mathematical operation of convolution. For our model $E_n = E * K_3/(K_2 + K_3)$. This expression has a simple interpretation, i.e., E is the probability that a BMHA molecule will leave the blood on a single capillary transit, $K_3/(K_2 + K_3)$ is the probability that a BMHA molecule entering the tissue will be metabolically trapped. No assumptions were made in the derivation of the operational equation limiting the value of E, other than it be in the range 0–1. It should also be noted that the operational equation is formally the same as the Sokoloff model of deoxyglucose metabolism.

Analysis of the operational equation shows that as t approaches infinity, the plateau concentration (C_{pl}) is given by $F * E_n * I$. Thus, the tissue concentration at the plateau is directly proportional to the "analog metabolism," a result likely to be of direct

clinical importance. Under these circumstances, $E_n(BMHA)$ can be calculated using the relation:

$$E_n(BMHA) = C_{pl}/[F * \int_0^\infty C_a(t)\, dt].$$

ACKNOWLEDGMENT

REFERENCES

1. Okada RD, Boucher CA, Strauss HW, Pohost GM. Exercise radionuclide imaging approaches to coronary artery disease. Am J Cardiol 1980;46:1188–1204.
2. Pohost GM, Alpert NM, Ingwall JS, Strauss HW. Thallium redistribution: mechanism and clinical utility. Semin Nucl Med 1980;11:70–93.
3. Liu P, Kiess MC, Okada RD, et al. The persistent defect on exercise thallium imaging and its fate after myocardial revascularization: does it represent scar or ischemia? Am Heart J 1985;110:996–1001.
4. Rocco TP, Dilsizian V, McKusick KA, Fischman AJ, Boucher CA, Strauss HW. Comparison of thallium redistribution with rest re-injection imaging for the detection of myocardial ischemia. Am J Cardiol 1990;66:158–163.
5. Bateman TM, Maddahi J, Gray RJ, et al. Diffuse slow washout of myocardial thallium-201: a new scintigraphic indicator of extensive coronary artery disease. J Am Coll Cardiol 1984;4:55–64.
6. Heyndrickx GR, Millard RW, McRitchie RJ, Maroko PR, Vatner SF. Regional ventricular function and electrophysiological alterations after brief coronary occlusion in conscious dogs. J Clin Invest 1975;56:978–985.
7. Braunwald E, Kloner RA. The stunned myocardium. Prolonged post ischemic ventricular dysfunction. Circulation 1983;66:1146–1149.
8. Greenberg JM, Murphy JH, Okada RD, Pohost GM, Strauss HW, Boucher CA. Value and limitations of radionuclide angiography in determining the cause of reduced left ventricular ejection fraction: comparison of idiopathic dilated cardiomyopathy and coronary artery disease. Am J Cardiol 1985;55:541–544.
9. Kaul S, Boucher CA, Newell JB, et al. Determination of quantitative thallium imaging variables that optimize detection of coronary artery disease. J Am Coll Cardiol 1986;7:527–537.
10. Schelbert HR. Positron emission tomography for the assessment of myocardial viability. Circulation 1991;84:1122–1131.
11. Hicks RJ, Herman WH, Kalff V, et al. Quantitative evaluation of regional substrate metabolism in the human heart by positron emission tomography. J Am Coll Cardiol 1991;18:101–111.
12. Neely JR, Revetto MJ, Oram JF. Myocardial utilization of carbohydrates and lipids. Prog in Cardiovasc Dis 1972;15:289–329.
13. Zierler KL. Fatty acids as substrates for heart and skeletal muscle. Circ Res 1976;38:459–463.
14. Opie LH. Effects of regional ischemia on metabolism of glucose and fatty acids. Circ Res 1976;38(suppl I):52–77.
15. Liedtke AJ. Alterations of carbohydrate and lipid metabolism in the acutely ischemic heart. Prog Cardiovasc Dis 1981;23:321–336.
16. Harris P, Glosterr JA, Ward B. Transport of fatty acids in the heart. Arch Mal Coeur Vaiss 1980;73:593–598.
17. Rose CP, Goresky CA. Constraints on the uptake of labeled palmitate by the heart. The barriers at the capillary and sarcolemmal surfaces and the control of intracellular sequestration. Circ Res 1977;41:534–545.
18. Bassingthwaighte JB, Noodleman L, van der Vusse G, Glantz JF. Modeling of palmitate transport in the heart. Moll Cell Biochem 1989;24:51–58.
19. Klein MS, Goldstein RA, Welch MJ, Sobel BE. External assessment of myocardial metabolism with [^{11}C]palmitate in rabbit hearts. Am J Physiol 1979;237:H51–H58.
20. Weiss ES, Ahmed SA, Welch MJ, Williamson JR, Ter-Pogossian MM, Sobel BE. Quantification of infarction in cross sections of canine myocardium in vivo with positron emission transaxial tomography and ^{11}C-palmitate. Circulation 1977;55:66–73.
21. Schon HR, Schelbert HR, Najafi A, et al. C-11 labeled palmitic acid for the noninvasive evaluation of regional myocardial fatty acid metabolism with positron computed tomography. I. Kinetics of C-11 palmitic acid in normal myocardium. Am Heart J 1982;103:532–547.
22. Schelbert HR, Henze E, Schon HR, et al. C-11 palmitate for the noninvasive evaluation of regional myocardial fatty acid metabolism with positron computed tomography. III. In vivo demonstration of the effects of the

substrate availability on myocardial metabolism. *Am Heart J* 1983;105:492–504.

23. Raichle ME, Welch MJ, Grubb RT Jr, et al. Measurement of regional substrate utilization rates by emission tomography. *Science* 1978;199:986–987.

24. Goldstein RA, Klein MS, Welch MJ, et al. External assessment of myocardial metabolism with C-11 palmitate in vivo. *J Nucl Med* 1980;21:342–348.

25. Schon HR, Schelbert HR, Najafi A, et al. C-11 labeled palmitic acid for the noninvasive evaluation of regional myocardial fatty acid metabolism with positron computed tomography. II. Kinetics of C-11 palmitic acid in acutely ischemic myocardium. *Am Heart J* 1982;103:548–561.

26. Ter-Pogossian MM, Klein MS, Markham J, et al. Regional assessment of myocardial metabolic integrity in vivo by positron-emission tomography with ^{11}C-labeled palmitate. *Circulation* 1980;61:242–255.

27. Livni E, Elmaleh DR, Levy S, Brownell GL, Strauss HW. ^{11}C-Labeled betamethylheptadecanoic acid: A new approach for assessing myocardial tracers for positron tomography. *J Nucl Med* 1982;23:169–175.

28. Elmaleh DR, Livni E, Levy S, Varnum D, Strauss HW, Brownell GL. Comparison of ^{11}C and ^{14}C-labeled fatty acids and their betamethyl analogs. *Int J Nucl Med Biol* 1983;10:181–187.

29. Elmaleh DR, Livni E, Brownell GL, Strauss HW. Biochemical rationale for the use of fatty acid analogs as agents for studying myocardial metabolism. *Proc Int Symp on Myocardial Metabolism: Clinical Cardiology* 1986.

30. Strauss HW, Livni E, Brill B, et al. In vivo studies of branched chain fatty acids. *Proc Int'l Symp on Myocardial Metabolism: Clinical Cardiology* 1986.

31. Fox KA, Abendschein DR, Ambos HD, Sobel BE, Bergmann SR. Efflux of metabolized and nonmetabolized fatty acid from canine myocardium. Implications for quantifying myocardial metabolism tomographically. *Circ Res* 1975;57:232–243.

32. Abendschein DR, Fox KA, Ambos HD, Sobel BE, Bergmann SR. Metabolism of beta-methyl [1-^{11}C] heptadecanoic acid in canine myocardium. *Int J Rad Appl Instrum* [B] 1987;16:579–585.

33. Humbert T, Keriel C, Batlle DM, Luu-Duc C, Comet M, Cuchet P. Intramyocardial fate of 15-p-iodophenyl-beta-methylpentadecanoic acid (IMPPA): is it a good tracer of fatty acid myocardial uptake? *Mol Cell Biochem* 1989;88:195–200.

34. Heymann MA, Payne BD, Hoffman JIE, Rodolph AN. Blood flow measurement with radionuclide labeled particles. *Prog Cardiovasc Dis* 1977;20:55–79.

35. Fink GD, Montgomery JA, France D, et al. Metabolism of beta-methyl-heptadecanoic acid in the perfused rat heart and liver. *J Nucl Med* 1990;31:1823–1830.

36. Litton J, Bergstrom M, Ericksson L, Bohm C, Blomquist G. Performance study of the PC-384 PET camera for the brain. *J Comput Assist Tomogr* 1984;8:74–87.

ERRATUM

Due to a production error, Figures 1 and 2 in the February 1994 First Impressions were printed incorrectly. The corrected figures and text are shown below.

FIRST IMPRESSIONS

A pinhole pertechnetate thyroid scan of a male with suspected Grave's disease.
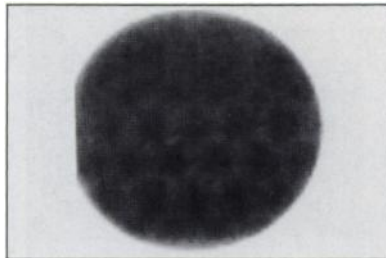

FIGURE 1.

FIGURE 2.

FIGURE 3.

PURPOSE

This 69-yr-old man was referred for evaluation of hyperthyroidism. The multinodular appearance on the initial study (Fig. 1) did not correlate with the smooth gland on palpation. A parallel-hole view on another camera demonstrated a gland consistent with Grave's disease (Fig. 2). A repeat "flood" revealed the reason for the discrepancy (Fig. 3).

TRACER

Technetium-99m-pertechnetate

ROUTE OF ADMINISTRATION

Intravenously

TIME AFTER INJECTION

20 minutes

INSTRUMENTATION

General Electric gamma camera; Siemens gamma camera

CONTRIBUTORS

A. Southee, P. Thomas and D. Front

INSTITUTION

Royal Newcastle Hospital, Newcastle, NSW, Australia